Supplemetary Figure 1.

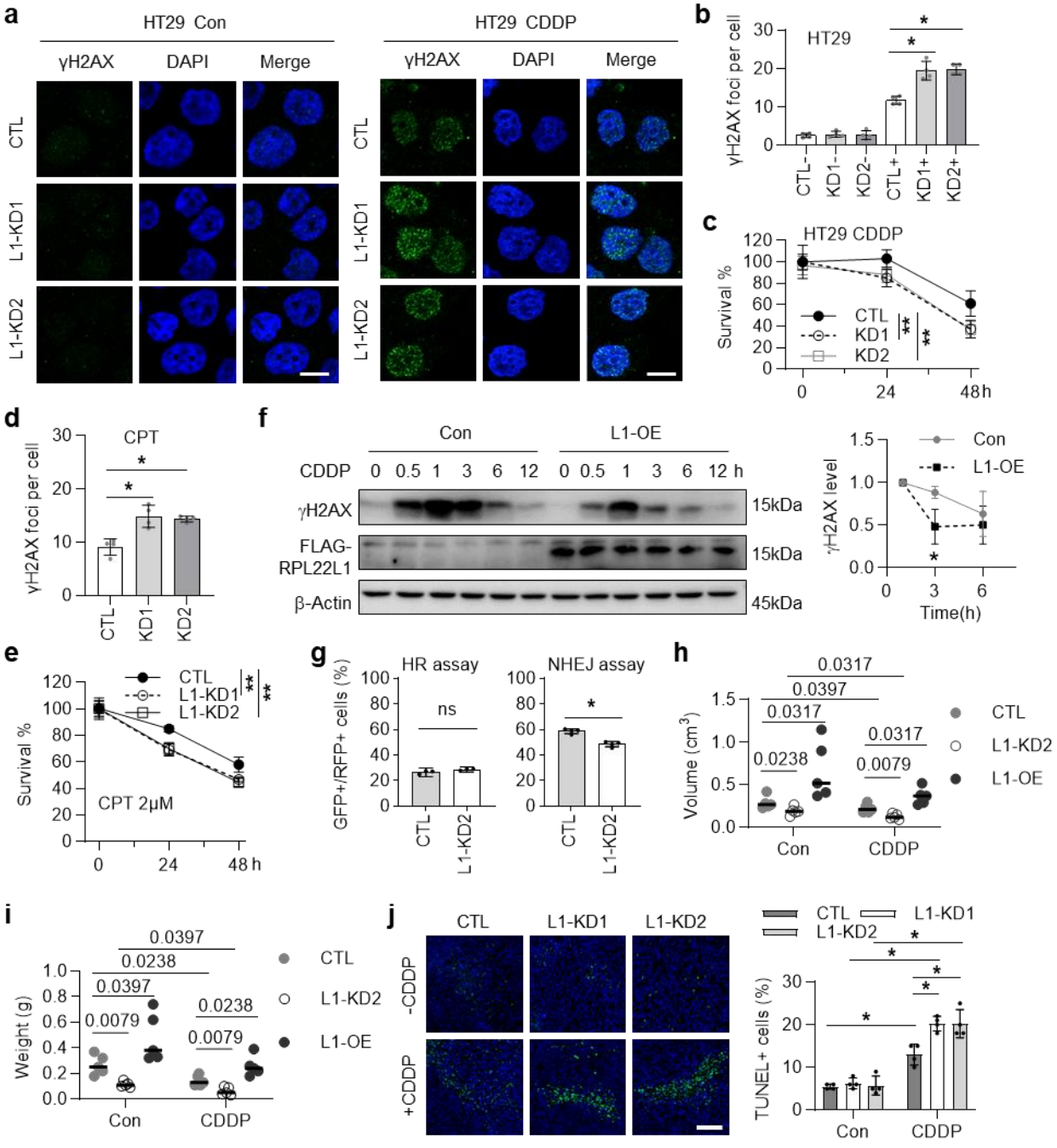

Supplemetary Figure 1. RPL22L1 promotes DNA repair and confers chemoresistance.
(a) Immunofluorescence staining of γH2AX foci in control (CTL) and RPL22L1 knockdown (L1-KD1 and L1-KD2) HT29 cells treated with or without 40 μM cisplatin for 12 hours. Nuclei were counterstained with DAPI. Scale bar, 10 μm. Four biological replicates were performed.
(b) Quantification of γH2AX foci per cell from (a). Each dot represents the mean number of foci per cell from one biological replicate (right). * $P = 0.0286$ (mean ± SD, 4 biological replicates, two-sided

Wilcoxon rank-sum test).
(c) Cell viability analysis of control and RPL22L1 knockdown HT29 cells following treatment with 40 μM cisplatin (CDDP). Data at the 24-hour time point were used for statistical analysis. ** $P = 0.0079$ (mean ± SD, 5 biological replicates, two-sided Wilcoxon rank-sum test).
(d) Quantification of γH2AX foci per cell from control and RPL22L1 knockdown RKO cells treated with camptothecin (CPT, 1 μM for 1 hour). Each point represents the mean number of foci per cell from one biological replicate. * $P = 0.0286$ (mean ± SD, 4 biological replicates, two-sided Wilcoxon rank-sum test).
(e) Cell viability analysis of control and RPL22L1 knockdown RKO cells following treatment with CPT. Data at the 24-hour time point were used for statistical analysis. ** $P = 0.0079$ (mean ± SD, 5 biological replicates, two-sided Wilcoxon rank-sum test).
(f) DNA repair kinetics indicating enhanced repair capacity in RPL22L1-overexpressing (L1-OE) cells. γH2AX levels were measured at multiple time points following cisplatin treatment and normalized to the 1 h time point. The samples derive from the same experiment but different gels for RPL22L1 and β-actin, and another for γH2AX were processed in parallel. Normalized γH2AX levels are shown on the right. * $P = 0.0329$ (Two-sided student's t-test, 3 biological replicates).
(g) Statistical analysis of HR- or NHEJ-mediated DNA repair efficiencies from control and RPL22L1 knockdown (L1-KD2) cells. ns, not significant ($P = 0.1$); * $P = 0.0286$ (mean ± SD, 4 biological replicates, two-sided Wilcoxon rank-sum test).
(h, i) Quantification of the tumor volume (h) and tumor weight (i) in control, RPL22L1 knockdown (L1-KD2), and RPL22L1 overexpression (L1-OE) groups with or without CDDP treatment. (mean ± SD, two-sided Wilcoxon rank-sum test, 5 biological replicates).
(j) Representative images of TUNEL staining in xenograft tumor tissues derived from control or RPL22L1-knockdown groups treated with or without cisplatin. Scale bar, 100 μm. The statistics of TUNEL-positive cells are shown on the right. * $P = 0.0286$ (mean ± SD, 4 biological replicates, two-sided Wilcoxon rank-sum test).

Supplemetary Figure 2.

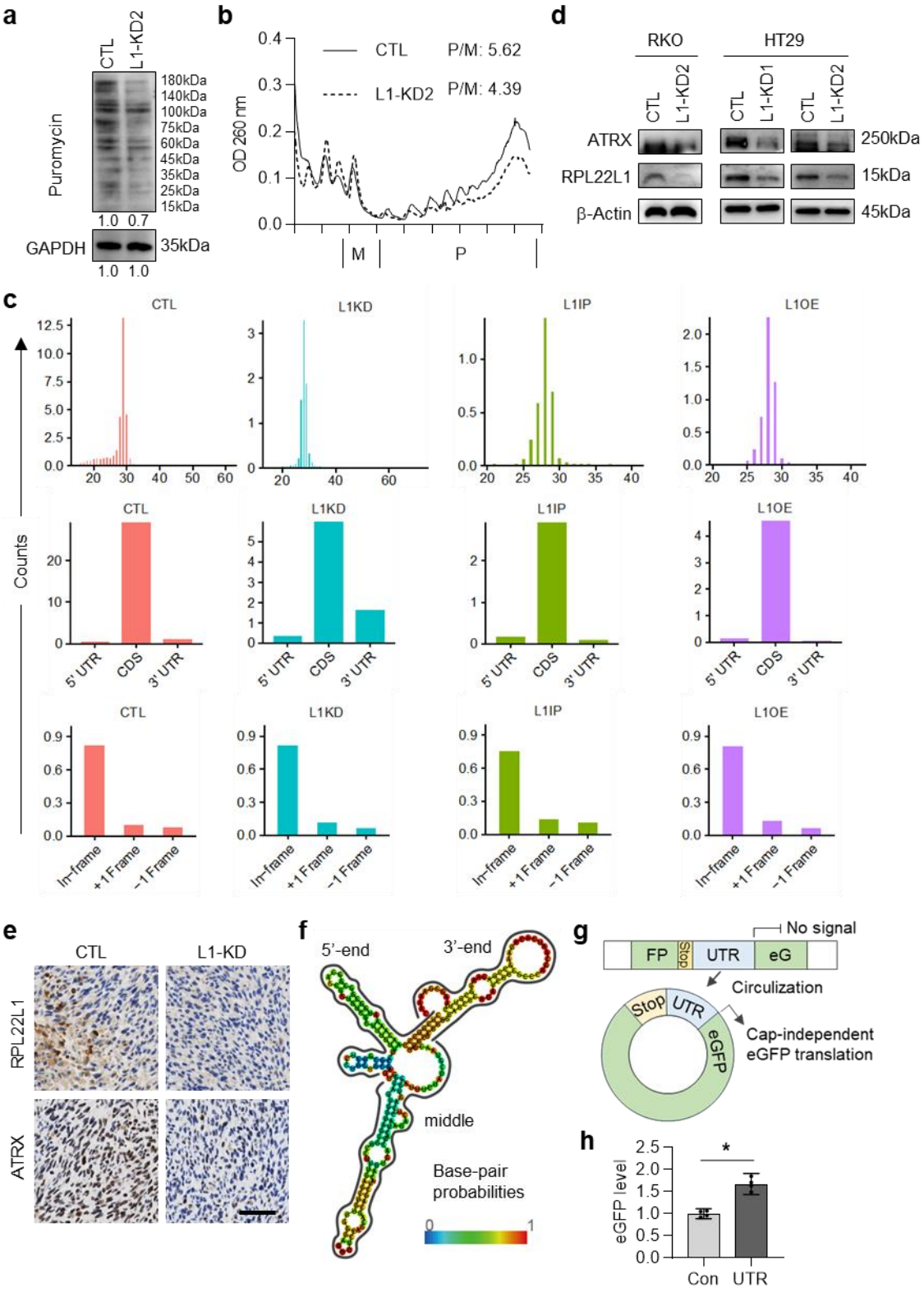

Supplemetary Figure 2. RPL22L1 regulates ATRX translation.

(a) Puromycin incorporation assay showing decreased global translation upon RPL22L1 knockdown (L1-KD2). GAPDH served as a loading control. The experiment was independently repeated three times with similar results.
(b) Sucrose gradient showing a shift from heavy to lighter polysome fractions in RPL22L1-depleted cells (L1-KD2). P: polysome; M: monosome.
(c) Quality analysis of Ribo-seq data. Reads length, distribution of RPF reads in regions, and each frame of mRNAs are shown.
(d) Immunoblot analysis of ATRX protein level in control (CTL) and RPL22L1 knockdown (L1-KD) cells. The experiment was independently repeated three times with similar results.
(e) Representative images of immunohistochemical staining for RPL22L1 and ATRX in xenograft tumor tissues derived from control and RPL22L1-knockdown groups following cisplatin treatment. Scale bar, 40 μm. The images are representative of two independent biological replicates.
(f) Predicted minimum free-energy (MFE) secondary structure of the *ATRX* 5'UTR, color-coded by base-pairing probability. The three regions used to generate the deletion mutants (5' end, middle, and 3' end) are highlighted.
(g) Schematic of a circular RNA-based assay for cap-independent translation.
(h) Relative eGFP expression of the reporter with *ATRX* 5'UTR. The empty vector control (Con) was normalized to 1. * $P = 0.0286$ (mean ± SD, 4 biological replicates, two-sided Wilcoxon rank-sum test).

Supplemetary Figure 3.

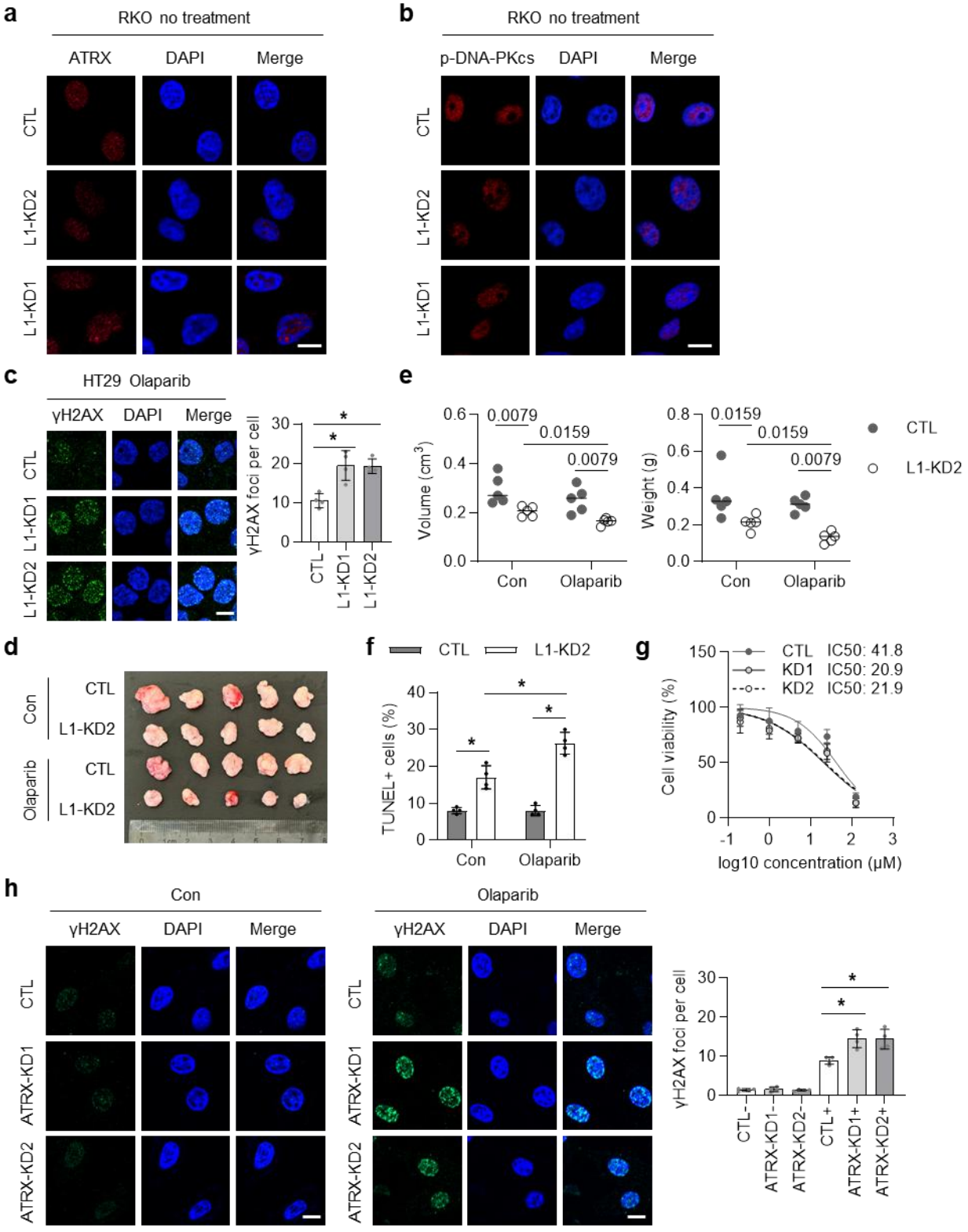

Supplemetary Figure 3. RPL22L1 and ATRX regulate DNA damage and olaparib sensitivity in

CRC cells.

(a, b) Immunofluorescence staining of ATRX (a) and p-DNA-PKcs (b) in RKO cells without cisplatin treatment. The images are representative of two independent biological replicates.

(c) Immunofluorescence staining of γH2AX in control (CTL) and RPL22L1 knockdown (L1-KD1 and L1-KD2) HT29 cells treated with olaparib (10 μM). Scale bar, 10 μm. Quantification of γH2AX foci per cell is shown on the right. Each point represents the mean number of foci per cell from one biological replicate. * $P = 0.0286$ (mean ± SD, 4 biological replicates, two-sided Wilcoxon rank-sum test).

(d) Representative images of tumors from control and RPL22L1 knockdown (L1-KD2) groups with or without olaparib treatment (50 mg/kg/day, 5 days).

(e) Quantification of the tumor volume and tumor weight in (d). (mean ± SD, two-sided Wilcoxon rank-sum test, 5 biological replicates).

(f) Quantification of TUNEL-positive cells. ns, not significant; * $P = 0.0286$ (mean ± SD, 4 biological replicates, two-sided Wilcoxon rank-sum test).

(g) Cell viability assays showing that ATRX depletion sensitizes RKO cells to olaparib. Data represent mean ± SD from 5 biological replicates. The calculated IC50 values were indicated.

(h) Immunofluorescence staining of γH2AX in control (CTL) and ATRX knockdown RKO cells treated with olaparib (10 μM). Scale bar, 10 μm. Quantification of γH2AX foci per cell is shown on the right. Each point represents the mean number of foci per cell from one biological replicate. Data represent mean ± SD from 4 biological replicates. * $P = 0.0286$ (two-sided Wilcoxon rank-sum test).

Supplementary Table 1.

Term	Genes	Count	List Total	Pop Hits	P-Value	Benjamini	Fold Enrichment	Bonferroni	FDR	Fisher Exact
DNA replication	0.02	11	213	36	1.05E-08	2.4E-06	12.24	2.4E-06	2.32E-06	6.29E-10
Base excision repair	0.02	11	213	44	8.59E-08	9.84E-06	10.02	1.97E-05	9.54E-06	6.74E-09
Spliceosome	0.04	20	213	217	1.7E-06	9.98E-05	3.69	0.000389	9.67E-05	4.25E-07
Cell cycle	0.03	17	213	158	1.74E-06	9.98E-05	4.31	0.000399	9.67E-05	3.67E-07
Mismatch repair	0.01	6	213	23	0.000211	0.00847	10.45	0.0471	0.00821	1.59E-05
Non-homologous end-joining	0.01	5	213	13	0.000222	0.00847	15.41	0.0496	0.00821	1.01E-05
Nucleotide excision repair	0.02	8	213	63	0.000899	0.0294	5.09	0.186	0.0285	0.000157
Nucleocytoplasmic transport	0.02	10	213	108	0.00142	0.0406	3.71	0.277	0.0393	0.000349

Supplementary Table 2.

RT-qPCR Oligos	
GAPDH-F	ATGGCAAATTCCATGGCACC
GAPDH-R	GACTCCACGACGTACTCAGC
β-actin-F	CACCATTGGCAATGAGCGGTTC
β-actin-R	AGGTCTTTGCGGATGTCCACGT
RPL22L1-F	CCTGCTTTGTAGGCACCAGA
RPL22L1-R	GTTGGGGTAGGGGCTTTTGA
ATRX-F	CCAGAGCCAGTGCTGAATGA
ATRX-R	ATGAAGCCCATCTTCTCCGC
shRNA Oligos	
shRPL22L1-1	GAGGTCAACCTGGAGGTTTAA
shRPL22L1-2	CATTGAACGCTTCAAGAATAA
shATRX-1	CGACAGAAACTAACCCTGTAA
shATRX-2	CCGGTGGTGAACATAAGAAAT